Supporting information

High reaction activity of nitrogen-doped carbon nanotube toward the electrooxidation of nitric oxide

Xuan Xu,[†] Lijun Yang,[‡] Shujuan Jiang,[‡] Zheng Hu,[‡] and Songqin Liu[†,*]

School of Chemistry and Chemical Engineering, Southeast University, Nanjing, 210096, P. R. China

Key Laboratory of Mesoscopic Chemistry of MOE, School of Chemistry and Chemical Engineering, Nanjing University, Nanjing, 210093, China

EXPERIMENTAL SECTION

Reagents. NCNTs with nitrogen-content of 3~5% were synthesized by chemical vapor deposition at 650 ^{o}C and pyridine was employed as precursor.[11] The as-prepared NCNTs were sequential refluxed in 6 M NaOH and 6 M HCl aqueous solution at 110 ^{o}C for 4 h in turn to remove the Al_2O_3 support and metal catalysts, respectively. The purified NCNTs were thoroughly washed with distilled water until the pH value of the filtrate reached 7, and then dried at 70 ^{o}C overnight for further study. CNTs were obtained from Shenzhen Nanotech Port Ltd. Co. (Shenzhen, China), consisting of CNTs with diameter of 10-20 nm and purity of ~95%. Well-dispersed NCNTs or CNTs suspension in ethanol with the concentration of 2 mg/mL was prepared under sonication for 30 min. Sodium nitrite (purity ≥99%) was purchased from Shanghai Chemical Reagent Ltd. Co. (Shanghai, China). 0.1 M pH 7.4 phosphate buffer solution (PBS) was prepared by mixing the stock solution of Na_2HPO_4 and NaH_2PO_4. Distilled water was used throughout the study.

Preparation of Nitric Oxide (NO) Solution. NO was generated according to previously reports.[S1] Briefly, 1.5 M H_2SO_4 was slowly dropped into a saturated $NaNO_2$ solution. The production gas was drived into a washing bottle which full of 5 M sodium hydroxide and collected with 0.1 M pH 7.4 deoxygenated PBS to obtain its saturated solution. The concentration of NO saturated solution was 2 mM at 20 ^{o}C determined with UV-Vis spectrophotometry with neutral Griess-Saltzman reagents. NO standard solutions were prepared by making successive dilutions of saturated NO solution. All the solutions were made fresh prior to each experiment.

Instrument. Electrochemical measurements were performed on a computer-controlled electrochemical analyzer (CHI 832B, CHI Instrument) with the conventional three-electrode

system composed of modified glassy carbon electrode (GC) as working electrode, platinum wire as counter electrode and saturated calomel electrode (SCE) as reference electrode in deoxygenated PBS at room remperature. A magnetic stirrer provided the convective transport during the amperometric measurement. The impedance experiment was carried out with frequencies ranging from 10 kHz to 0.01 Hz in a 0.1 M PBS 7.4 containing 0.53 mM NO. The data was recorded at + 0.7 V (vs. the open circuit potential) and fitted with an equivalent circuit R(C(RW)) for extraction of electrical parameters from the impedance spectra.

Electrode Preparation. The GC was successively polished using 1.0 and 0.3 μm alumina powder followed by rinsing thoroughly with doubly distilled water. After successive sonication in 1:1 nitric acid, acetone, and doubly distilled water, the electrode was rinsed with doubly distilled water and dried at room temperature. A 10 μL 2 mg/mL of NCNTs or CNTs suspension was dropped on the surface of the pretreated GC and dried under vacuum to obtain NCNT modified GC electrode (NCNT/GC) and CNT modified GC electrode (CNT/GC).

Fig S1. CVs of NCNTs/GC in 0.1 M pH 7.4 PBS containing 0.065 mM NO (a) and 1 mM NO_2^- at 10 mV/s

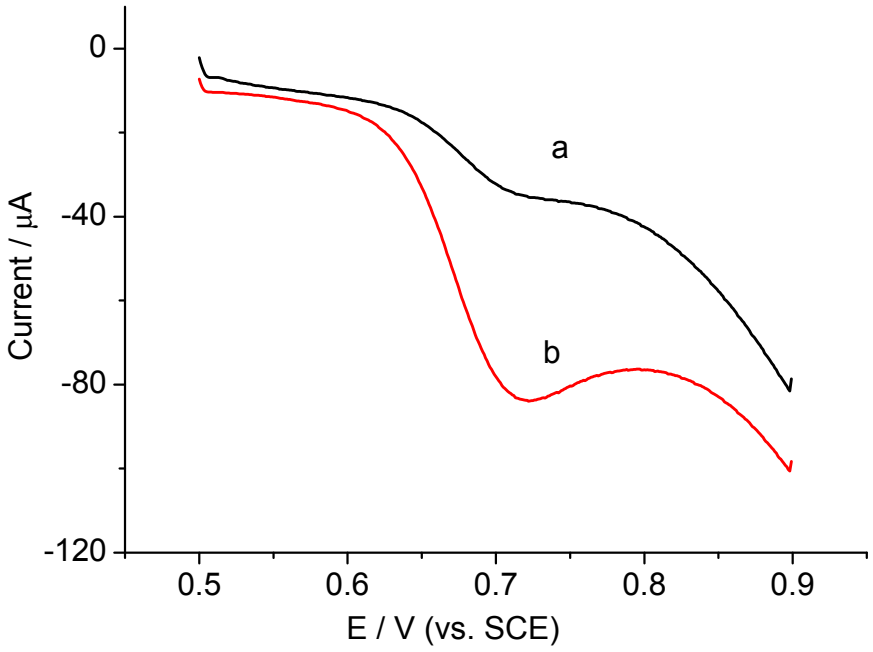

Along with the scan rate increased, the peak current increased and the peak potential shifted in positive direction, confirming the irreversible nature of the reaction process (Fig. S2). The peak currents of NO depend linearly on the corresponding square root of the potential scan rate in the range from 10 to 150 mV/s with a linear correlation coefficient of 0.995 for CNT/GC and 0.999 for NCNT/GC, respectively (inset in Fig. 2). Thus it can be concluded that the anodic oxidation processes of NO at two electrodes are diffusion-controlled.

Fig. S2 CV curves obtained at (A) NCNT/GC and (B) CNT/GC electrodes in 0.10 M pH 7.4 PBS in the presence of 0.169 mM NO removed oxygen with high purity of N_2 at different scan rates: 10, 30, 50, 70, 90, 110, 130, 150 mV/s. (insert: Dependency of peak currents on the corresponding square root of scan rate)

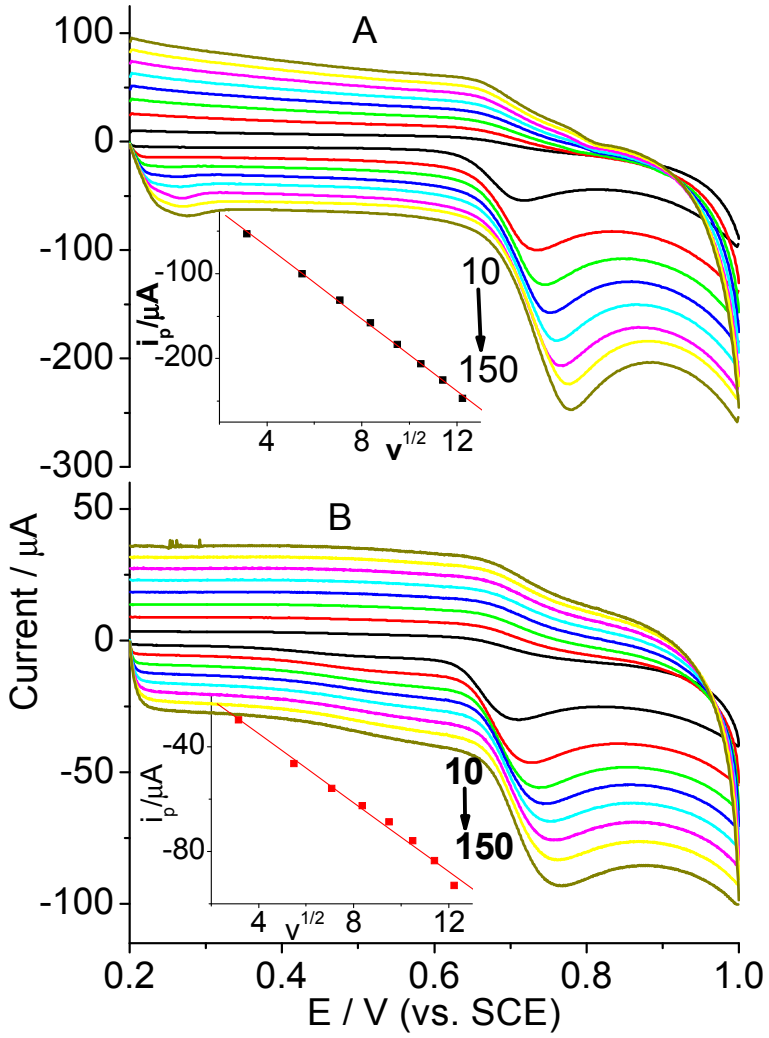

Standard rate constant k_s

For an irreversible diffusion-controlled process, the peak potential is proportion to ln(i_p) within the following equation.

$i_p = 0.227nFAC_o^* k_s \times \exp[(-\alpha nF/RT)(E_p - E^o)]$

where i_p, k_s, E^o are peak current, standard rate constant and formal potential (obtained from extrapolation of the peak current to the potential sweep rate of zero). Thus, a plot of ln(i_p) *vs*. (E_p - E^o) at different scan rates would be a straight line with a slope proportional to αn, and an intercept proportional to k_s (supporting information Fig. S3 and S4). With this method, the standard rate constant k_s for oxidation process (F = 96500 C/mol, A = 0.1256 cm^2, Co* = 0.169 mol/m^3) is 10.33×10^{-5} m/s and 6.67×10^{-5} m/s at NCNT/GC and CNT/GC, respectively. This further demonstrats that NCNTs enable faster electron-transfer kinetics for NO oxidation than that of CNTs.

Fig. S3 Plots of ln(i_p) vs (E_p-E^o) on CNTs modified electrode.

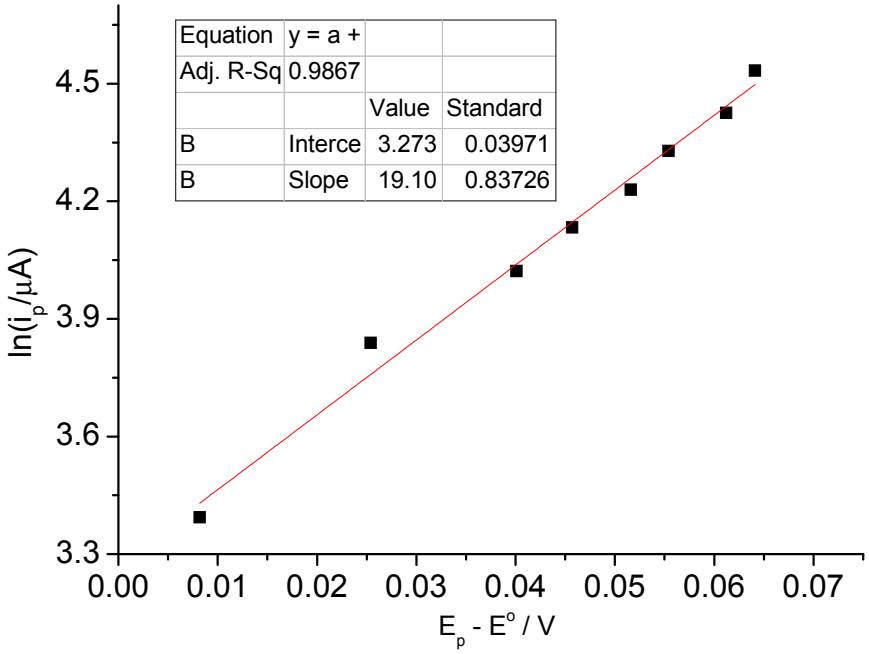

Fig. S4 Plots of $\ln(i_p)$ vs (E_p-E^o) on NCNTs modified electrode.

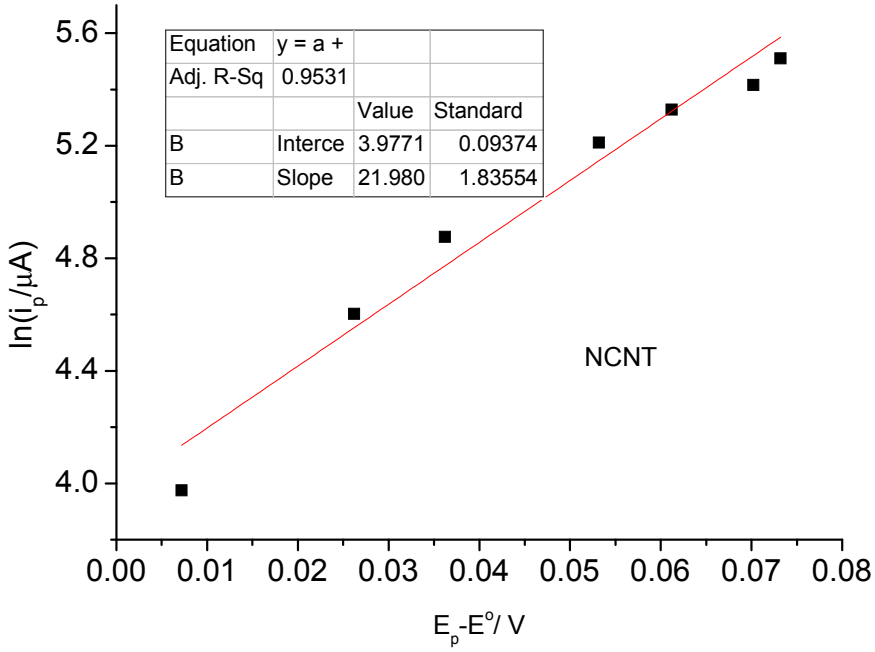

Calculation settings

Metallic armchair (5,5) single-walled carbon nanotube with length of 5 unit cells and diameter of 6.85 Å was used in the theoretical calculations. Graphitic NCNT(5,5) (gNCNT(5,5)) was modeled by substituting a center carbon atom with nitrogen; pyridinic NCNT(5,5) (pNCNT(,5,5)) was formed by removing a central C atom among three hexagons and replacing the three surrounding C atoms with three N atoms. The terminal sites of the NCNT(5,5) were saturated with hydrogen atoms in order to avoid the edge effect.

Theoretical calculations based on DFT were carried out with Gaussian09 package (ref 16b in the text). The geometrical optimizations were performed using unrestricted DFT method with Becke's hybrid three parameter nonlocal exchange functional combined with the Lee-Yang-Parr gradient corrected correlation functional (B3LYP)[S2,S3]. The 6-31G (d,p) basis set was employed for all the elements. NBO analysis was investigated at the same theoretical level with NBO 3.1(ref 16d in the text) embedded in Gaussian 09. The spin multiplicity corresponding to the lowest energy state was adopted in the calculations. The adsorption energy (E_{ads}) for a NO on NCNT(5,5) was calculated as follow:

$$E_{ads}=E(\mathrm{NT+NO}) - E(\mathrm{NT}) - E(\mathrm{NO}) \quad (1)$$

Where E(NT+NO), E(NT) and E(NO) is the energy of the NO-NCNT(5,5) system, the relaxed NCNT(5,5) and the isolated triplet molecular oxygen, respectively.

Fig. S5 Optimum the detection potential. Plots of steady-current vs. the applied potential before (a) and after (b) addition of 0.0186 mM NO. C is the difference of the steady-current on NCNTs/GC before and after addition of NO.

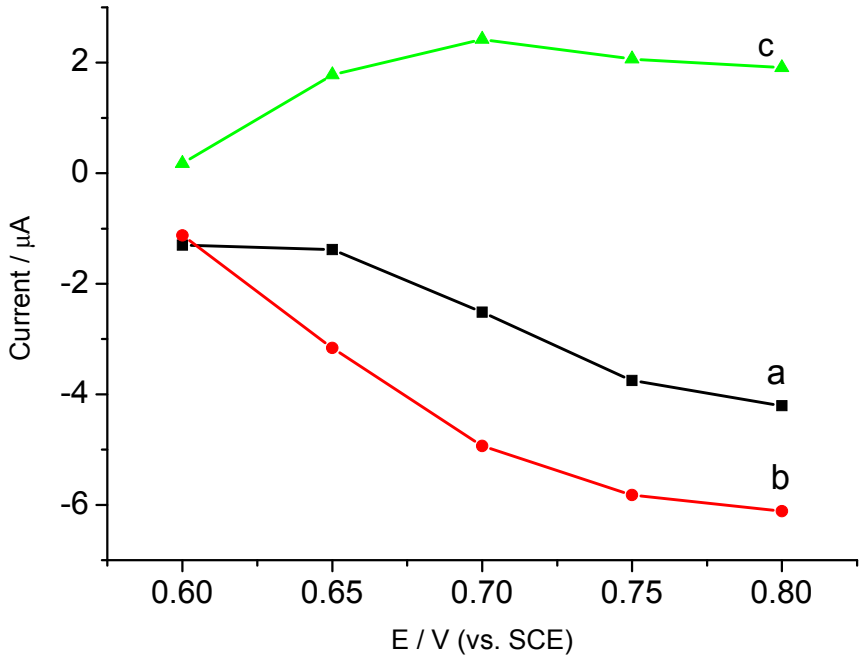

Fig. S6 NCNT/GC and NCNT-Nafion/GC electrodes with successive addition of AA, $NaNO_2$, NO (indicated by arrows for marked concentrations) in 0.10 M pH 7.4 PBS at an applied potential of +0.7 V (vs. SCE).

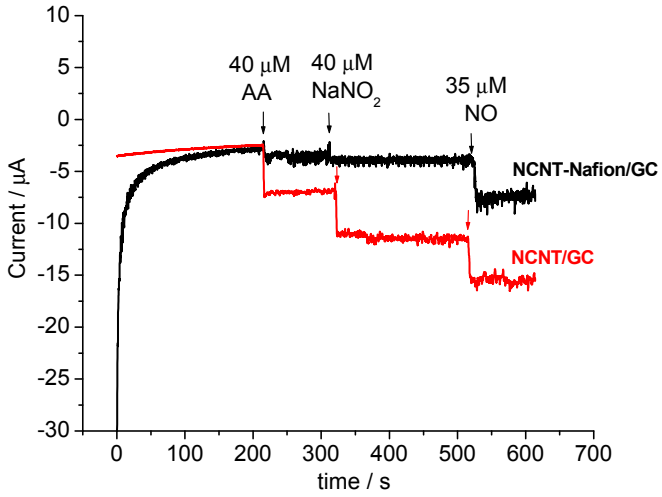

Nitrite and ascorbic acid (AA) was found to interfere the electrooxidative measurement in the presented work. The current changed dramatically when 40 μM nitrite or 40 μM AA was added into the solution and their sensitivities are almost as high as NO. However, these interferes could be avoided by coating a Nafion film on NCNT surface. After 5 μL 0.5% Nafion aqueous solution was covered on the electrode surface, the current for AA and nitrite decreased dramatically while no obviously change was observed from NO. As a result, possible interfering species influencing NO measurement can be overcome.

Reference

S1 (a) N. Diab, J. Oni and W. Schuhmann, *Bioelectrochemistry*, 2005, **66**, 105-110. (b) C. M. Li, J. F. Zang, D. P. Zhan, W. Chen, Q. S. Chang, A. L.Teo, Y. T. Chua, V. S. Lee and S. M. Moochhala, *Electroanalysis*, 2006, **18**, 713-718.

S2 A. D.Becke, *J. Chem. Phys.* 1993, **98,** 5648.

S3 P. J. Stephens, F. J. Devlin, C. F. Chabalowski, M. J. Frishch, *J. Phys. Chem*. 1994, **98**, 11623.

Complete reference of Ref 16b in the text

Gaussian 09, Revision A.1, M. J. Frisch, G. W. Trucks, H. B. Schlegel, G. E. Scuseria, M. A. Robb, J. R. Cheeseman, G. Scalmani, V. Barone, B. Mennucci, G. A. Petersson, H. Nakatsuji, M. Caricato, X. Li, H. P. Hratchian, A. F. Izmaylov, J. Bloino, G. Zheng, J. L. Sonnenberg, M. Hada, M. Ehara, K. Toyota, R. Fukuda, J. Hasegawa, M. Ishida, T. Nakajima, Y. Honda, O. Kitao, H. Nakai, T. Vreven, J. A. Montgomery, Jr., J. E. Peralta, F. Ogliaro, M. Bearpark, J. J. Heyd, E. Brothers, K. N. Kudin, V. N. Staroverov, R. Kobayashi, J. Normand, K. Raghavachari, A. Rendell, J. C. Burant, S. S. Iyengar, J. Tomasi, M. Cossi, N. Rega, J. M. Millam, M. Klene, J. E. Knox, J. B. Cross, V. Bakken, C. Adamo, J. Jaramillo, R. Gomperts, R. E. Stratmann, O. Yazyev, A. J. Austin, R. Cammi, C. Pomelli, J. W. Ochterski, R. L. Martin, K. Morokuma, V. G. Zakrzewski, G. A. Voth, P. Salvador, J. J. Dannenberg, S. Dapprich, A. D. Daniels, Ö. Farkas, J. B. Foresman, J. V. Ortiz, J. Cioslowski, and D. J. Fox, Gaussian, Inc., Wallingford CT, 2009.